Journal of Power Sources 189 (2009) 371–377

Contents lists available at ScienceDirect

Journal of Power Sources

journal homepage: www.elsevier.com/locate/jpowsour

Study on lithium/air secondary batteries—Stability of NASICON-type lithium ion conducting glass–ceramics with water

Satoshi Hasegawa, Nobuyuki Imanishi*, Tao Zhang, Jian Xie, Atsushi Hirano, Yasuo Takeda, Osamu Yamamoto

Department of Chemistry, Faculty of Engineering, Mie University, 1577 Kurimamachiya-cho, Tsu, Mie 514-8507, Japan

ARTICLE INFO

Article history:
Received 2 August 2008
Accepted 6 August 2008
Available online 14 August 2008

Keywords:
Lithium/air battery
Solid electrolyte
Solid lithium ion conductor
LiPON
Glass–ceramics

ABSTRACT

The water stability of the fast lithium ion conducting glass–ceramic electrolyte, $Li_{1+x+y}Al_xTi_{2-x}Si_yP_{3-y}O_{12}$ (LATP), has been examined in distilled water, and aqueous solutions of $LiNO_3$, LiCl, LiOH, and HCl. This glass–ceramics are stable in aqueous $LiNO_3$ and aqueous LiCl, and unstable in aqueous 0.1 M HCl and 1 M LiOH. In distilled water, the electrical conductivity slightly increases as a function of immersion time in water. The Li–Al/$Li_{3-x}PO_{4-y}N_y$/LATP/aqueous 1 M LiCl/Pt cell, where lithium phosphors oxynitrides $Li_{3-x}PO_{4-y}N_y$ (LiPON) are used to protect the direct reaction of Li and LATP, shows a stable open circuit voltage (OCV) of 3.64 V at 25 °C, and no cell resistance change for 1 week. Lithium phosphors oxynitride is effectively used as a protective layer to suppress the reaction between the LATP and Li metal. The water-stable Li/LiPON/LATP system can be used in Li/air secondary batteries with the air electrode containing water.

1. Introduction

Lithium/air batteries have potentially higher energy density, because the active cathode materials are supplied from outside of the battery. The theoretical specific energy density of lithium/air, excluding oxygen, is 11.140 kWh kg^{-1} which is comparable to that of a gasoline/air. To develop a high performance lithium/air secondary battery, a number of problems need to be resolved in relation to the electrolyte, the lithium anode, and the air cathode. Three types of electrolyte have been proposed, namely non-aqueous electrolytes [1,2], gel-type polymer electrolytes [3], and solid electrolytes [4]. Non-aqueous electrolytes and gel-type polymer electrolytes are both stable with lithium metal, however their instability to moisture from the air is an issue for long term operation [5]. Visco et al. [6] proposed an unique lithium/air cell with a water-stable lithium conducting solid electrolyte based on a NASICON-type $Li_3M_2(PO_4)_3$. This cell consisted of a lithium anode, the solid electrolyte described above, an oxygen electrode, and a reservoir to hold the cell reaction product. The authors reported stable discharge performance in the Li/solid electrolyte/aqueous 4 M NH_4Cl/Pt, air cell for nearly 2 months. $Li_{1+x}M_xTi_{2-x}(PO_4)_3$ (M = Al, Sc, Y and La), a NASICON-type lithium ion conducting solid electrolyte, has been reported by Aono et al. [7], and a maximum conductivity (10^{-3} S cm^{-1} at 300 K) was achieved at $x \approx 0.3$ for $Li_{1+x}Al_xTi_{2-x}(PO_4)_3$. The water stability of $Li_{1.3}Al_{0.3}Ti_{1.7}(PO_4)_3$ was further examined by Cretin et al. [8]. The authors found that the weight loss for the sample prepared by the sol–gel process after immersion for about 100 h in distilled water was approximately 0.9%. Thokchom and kumar [9] reported the water stability of the glass–ceramic system $Li_{1.3}Al_{0.3}Ti_{1.7}(PO_4)_3$, and observed a small degradation (slight buckling) of the membrane after 65 days of immersion in tap water. The conductivity data and any phase changes, however, after immersion in the water, were not reported. We have reported in our previous work that no significant change of the XRD patterns, and in the conductivity, were observed for the glass–ceramic system, $Li_{1+z+y}Al_xTi_{2-x}Si_yP_{3-y}O_{12}$ (LATP), after immersed in water for 1 month [10].

In this study, the stability of the LATP plate immersed in different types of aqueous electrolytes was examined. In addition, the stability of the Li/$Li_{3-x}PO_{4-y}N_y$/LATP/water cell was studied, where the $Li_{3-x}PO_{4-y}N_y$ (LiPON) layer was used to protect the reaction between the Li and the LATP. The Li/$Li_{3-x}PO_{4-y}N_y$/LATP system is attractive for the development of a durable lithium/air secondary battery, as it shows stability in moist air.

2. Experimental

The water-stable NASICON-type glass–ceramic $Li_{1+x+y}Al_xTi_{2-x}Si_yP_{3-y}O_{12}$ plate (150 μm in thickness and 3.05 g cm^{-3} in density) and powder (1–10 μm average particle diameter) were supplied by Ohara Inc., Japan. The preparation method of LATP has been

* Corresponding author. Tel.: +81 59 231 9420; fax: +81 59 231 9478.
E-mail address: imanishi@chem.mie-u.ac.jp (N. Imanishi).

0378-7753/$ – see front matter © 2008 Elsevier B.V. All rights reserved.
doi:10.1016/j.jpowsour.2008.08.009

described in the literature [11,12]. The water stability test of the LATP was carried out for the plate and the powder. The samples were immersed in distilled water; aqueous 1 M LiOH; aqueous 1 M $LiNO_3$; aqueous 1 M LiCl; and aqueous 0.1 M HCl all at 25 °C.

The impedances of the LATP plates, using sputtered gold electrodes, were measured using a Solartron 1260 frequency response analyzer with a Solartron 1287 electrochemical interface in the frequency range 0.1 Hz–1 MHz. *Z* plot software was employed for data analysis and presentation. The ac impedances of the samples in air were measured in the temperature range from 20 to 80 °C at 10 °C steps. At each temperature, the specimen was equilibrated for 20 min before the impedance measurement.

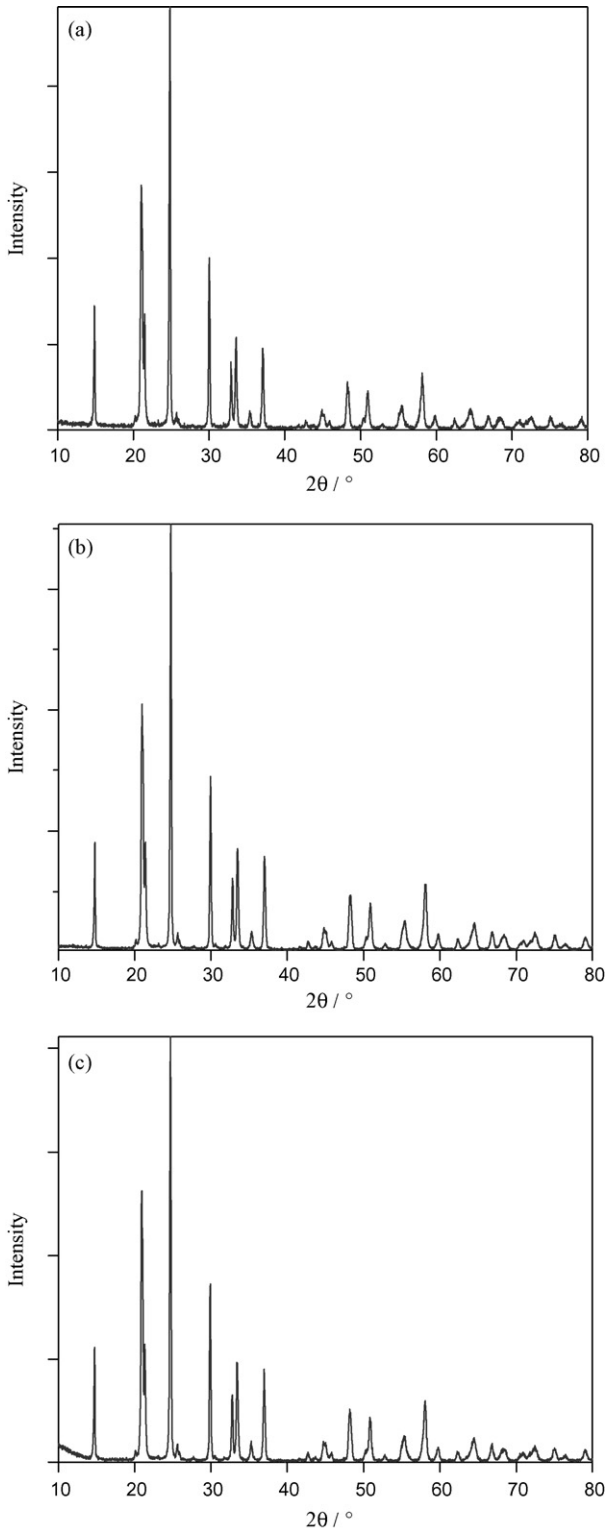

Fig. 1. XRD patterns of the LAPT plates immersed in distilled water for 1 month (a), for 8 months (b) and the pristine plate (c).

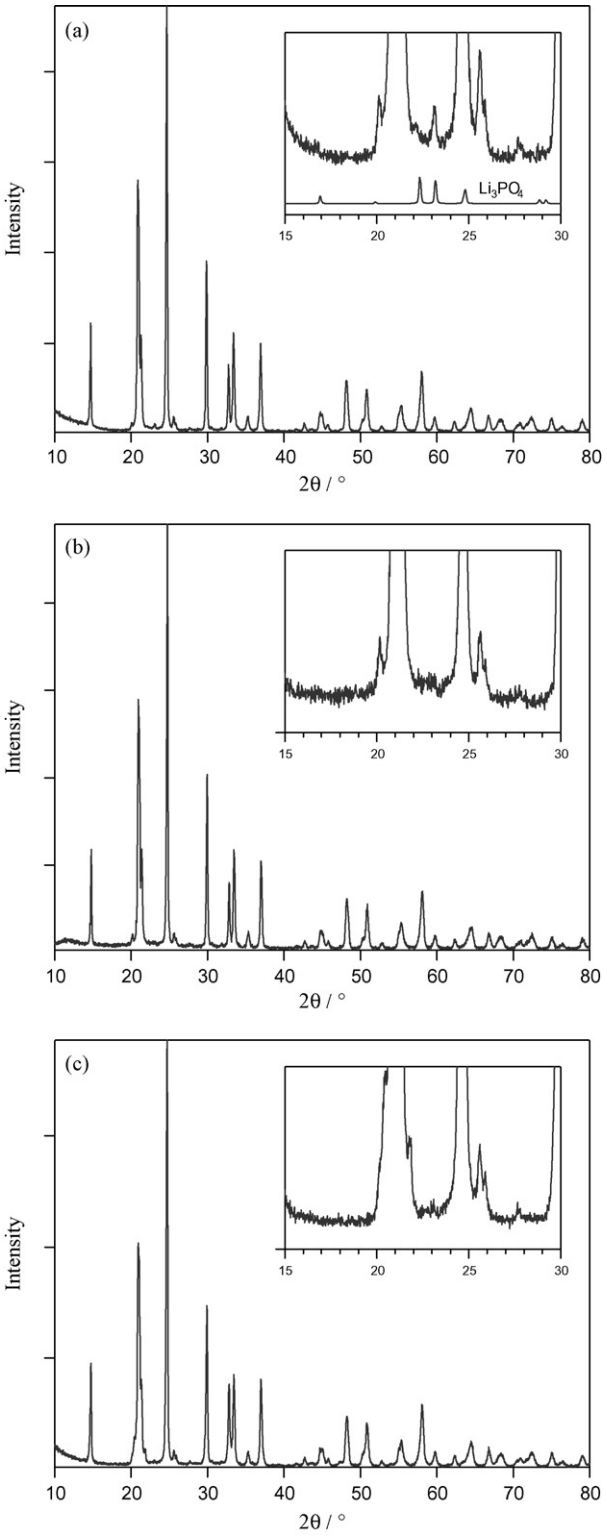

Fig. 2. XRD patterns of the LAPT plates immersed in 1 M LiOH solution for 1 week (a), 1 M $LiNO_3$ solution for 3 weeks (b) and 0.1 M HCl solution for 3 weeks (c).

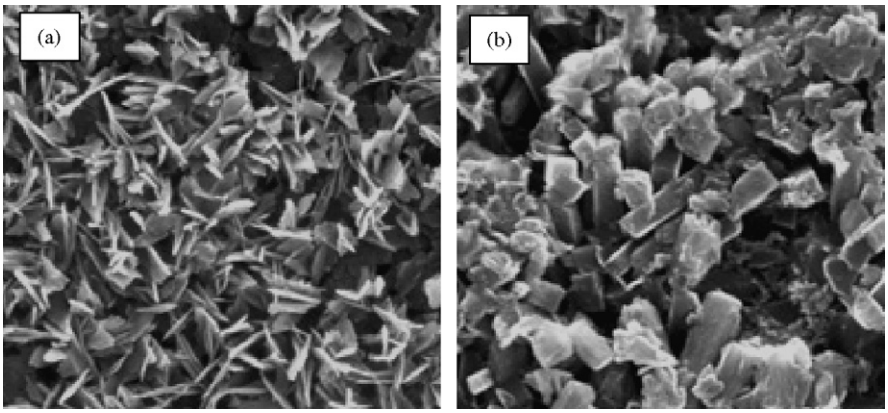

Fig. 3. SEM images of the LAPT plates immersed in 1 M LiOH for 1 week (a) and for 8 months (b).

X-ray diffraction (XRD) data were obtained using a Rigaku RINT 2500 with a copper target. Scanning electron microscope (SEM) images were measured using a Hitachi SEM S-4000.

The water stability test of the Li/LiPON/LATP cell was carried out using the 150-μm thick LATP plate, which had been prepared by the method previously reported [10]. On the LATP plate, a thin LATP film was sputtered to make good contact with the LiPON film. The LiPON thin film (thickness approximately 1 μm), which also served to stop the reaction between the Li and the LATP, was sputtered onto the LATP plate using a Li_3PO_4 target in a nitrogen gas flow. To make good contact between the LiPON and the Li metal, an Al thin film was sputtered on the LiPON surface. The Li–Al/LiPON/LATP cell was sealed using a plastic film, leaving a square window of 5 mm × 5 mm onto the plate, to make contact with the electrolyte solution. The cell was then immersed into the aqueous 1 M LiCl solution. Platinum plates, with a platinum black coating, were used as the counter and reference electrodes. The impedance of the cell was measured in a temperature range from 20 to 60 °C. A constant current was passed into the cell at 25 °C and the voltages between the Li metal electrode and the reference electrode were recorded.

3. Results and discussion

Fig. 1 shows the XRD patterns of the LATP plate immersed in distilled water at 25 °C. The LATP plates immersed in water for 1 month (a), and 8 months (b) and show no significant difference in their XRD

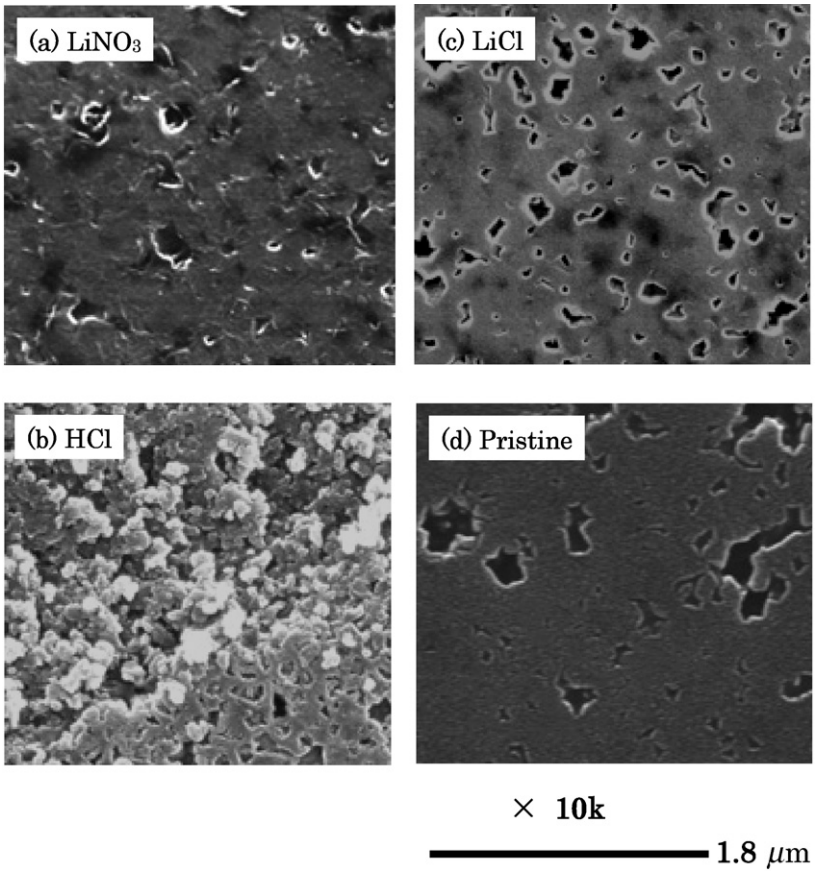

Fig. 4. SEM images of the LAPT plates immersed in 1 M $LiNO_3$ for 3 weeks (a), 1 M LiCl for 3 weeks (b), 0.1 M HCl for 3 weeks (c) and pristine plate (d).

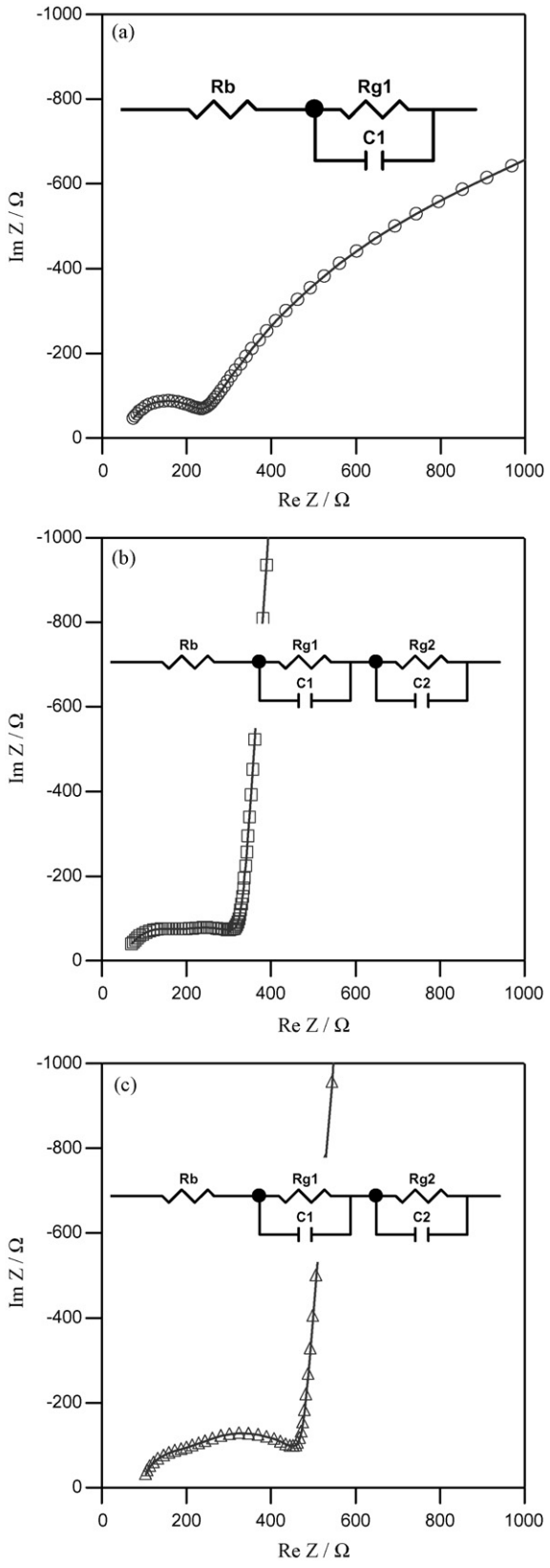

Fig. 5. Impedance spectra at 25 °C of the pristine LATP plate (a), the LATP plate immersed in distilled water for 1 month (b) and the LATP plate immersed in distilled water for 8 months (c).

patterns from the pristine LATP sample with the NASICON-type structure (c). These results suggest that the LATP plate is structurally stable for long periods of time in water. Fig. 2 shows the XRD patterns of the LATP plates immersed in aqueous 1 M LiOH for 1 week (a), aqueous 0.1 M HCl (pH ≈ 1) for 3 weeks (b) and 1 M aqueous $LiNO_3$ (pH ≈ 5.8) for 3 weeks (c). These XRD studies indicate that the LATP plate is stable in aqueous 1 M $LiNO_3$, but unstable in aqueous 1 M LiOH. The LATP plate immersed in aqueous1 M LiOH for 1 week gave an extra XRD diffraction peak at near 23° in 2θ, as shown in Fig. 2(a). The extra diffraction peak was indexed to the Li_3PO_4 phase. The LATP powder immersed in aqueous 0.1 M LiOH for 2 weeks showed no extra diffraction peaks. These results suggest that LATP cannot be used in strong alkaline media, but can be used in a weak alkaline solution for short periods of time. The XRD patterns of the LATP plate immersed in aqueous 0.1 M HCl show an unidentified extra peak at approximately 22° in 2θ. The XRD study for the LATP powder immersed in aqueous 5 M HCl showed a very different diffraction pattern from the starting structure after only 3 days. This is very relevant information from a practical standpoint for the NASICON-type glass–ceramics in lithium/air batteries, as strong acid and alkaline solutions cannot be used as electrolytes (or the reservoir of the reaction product) at the air electrode.

The decomposition of the LATP plate in the alkaline and acid solutions was also confirmed from the SEM images. Fig. 3 shows the SEM images of the LATP plates immersed in aqueous 1 M LiOH for 1 week (a) and 8 months (b). Significant changes of the surface morphology were observed for the sample immersed for 8 months. The glassy surface of the fresh LATP plate has changed to a rough one, meaning that the LATP plate reacts with LiOH. The SEM images of the LATP plates immersed in aqueous 1 M $LiNO_3$ (pH ≈ 5.8) for 1 week (a), in aqueous 1 M LiCl for 1 week (b), in aqueous 0.1 M HCl (pH ≈ 1) for 1 week (c) and the pristine LATP plate (d) are shown in Fig. 4. The surface morphology of the LATP plates immersed in aqueous 1 M $LiNO_3$ and aqueous 1 M LiCl show no change; however the plate immersed in aqueous 0.1 M HCl showed a significant morphological change on some parts of the plate. These surface morphology changes confirm the XRD results in Fig. 2.

The electrical conductivities of the LATP plate immersed in distilled water; aqueous 1 M $LiNO_3$; aqueous 0.1 M HCl; aqueous 1 M LiCl; and aqueous 1 M LiOH were examined in a temperature range from 25 to 80 °C. In a previous paper [10], we reported that the electrical conductivity of the LATP plate immersed in distilled water for 1 month had slightly decreased, and this decrease was explained by the formation of a second phase in the grain boundary. The ac impedance spectra of the pristine LATP and those of the LATP plates immersed in distilled water for 1 month and 8 months at 25 °C are shown in Fig. 5. The spectrum of the pristine LATP shows one semicircle plus a larger semicircle in the lower frequency range which appears as an electrode response. The smaller semicircle is attributed to the grain boundary resistance of the LATP. The intercept of the semicircle on the real axis at high frequency represents the bulk resistance of the LATP, R_b [13]. However, the samples immersed in water for 1 month and 8 months show a depressed semicircle. This change in response is due to the different grain boundary phases present in the sample due to the decomposition of the LATP plate in water. The grain boundary resistance slightly increases as a function of the immersion time in water. The results were analyzed using an equivalent circuit model shown in Fig. 5, in which two resistances for the different types of grain boundaries are assumed. The grain boundary resistance in the lower frequency range, R_{g2}, increases from 144 Ω for the sample immersed in water for 1 month to 242 Ω for that immersed in water for 8 months while in the high frequency range, R_{g1} is virtually constant of 135 Ω as a function of immersion time. These results show that R_{g1} is attributed to the grain boundary of the LATP plate, while R_{g2} can

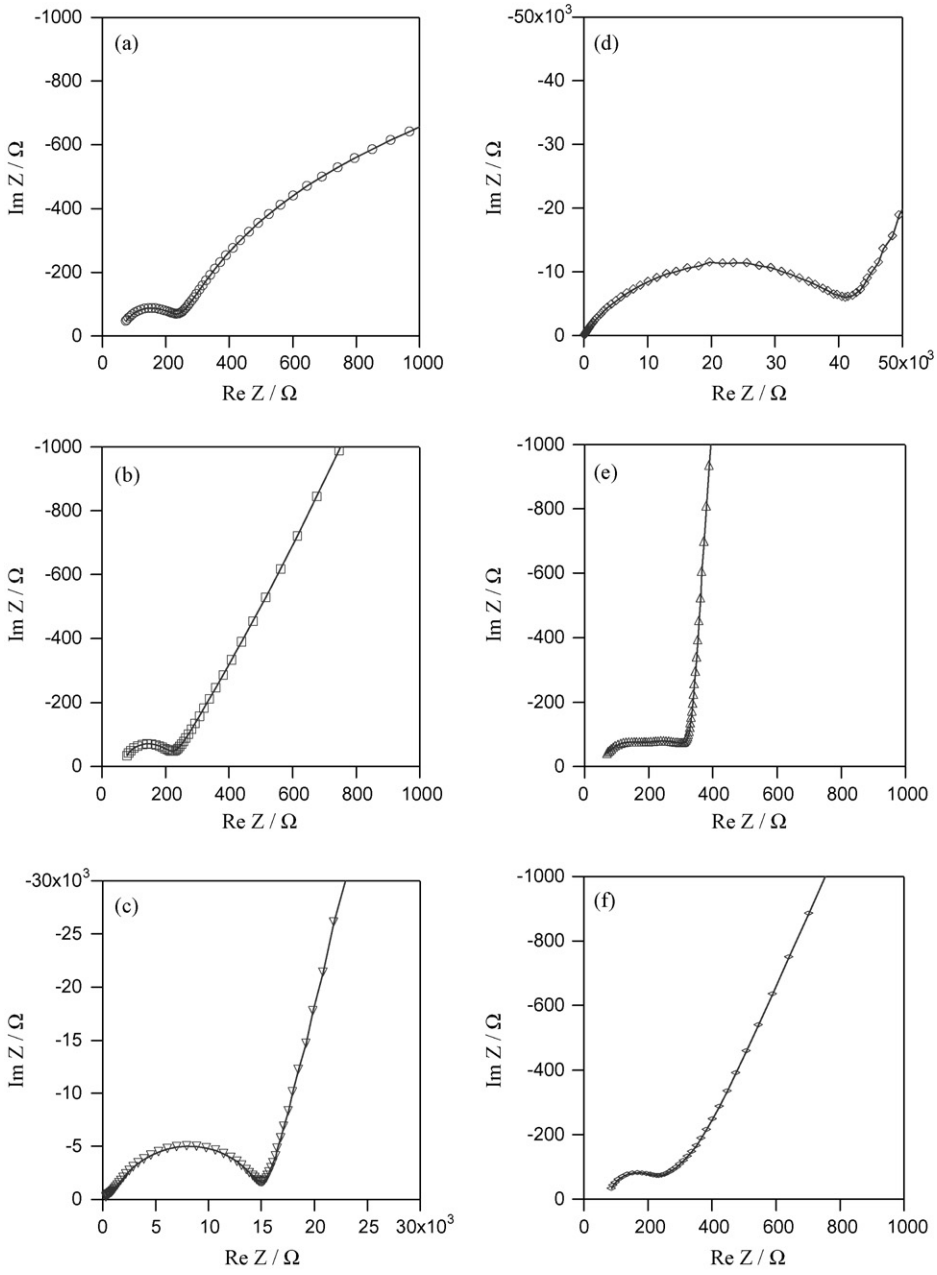

Fig. 6. Impedance spectra at 25 °C of the pristine LATP plate (a), the LATP plate immersed in 1 M $LiNO_3$ for 3 weeks (b), 0.1 M HCl for 3 weeks (c), 1 M LiOH for 8 months (d), distilled water for 1 month (e) and 1 M LiCl for 3 weeks (f).

be attributed to the formation of the second phase at the grain boundary due to the reaction of the LATP and water.

The impedance profiles of the LATP plates immersed in aqueous 1 M $LiNO_3$; aqueous 1 M LiOH; aqueous 0.1 M HCl; and aqueous 1 M LiCl, are shown together with the pristine LATP plate in Fig. 6. The impedance profiles of the samples immersed in aqueous $LiNO_3$ and aqueous LiCl are similar to the pristine LATP plate with no contributions from extra phases. This means that the LATP plate is electrochemically stable in aqueous $LiNO_3$ and aqueous LiCl. However, the resistances of the LATP plate immersed in aqueous 1 M LiOH and aqueous 0.1 M HCl drastically increased. These higher resistances are due to the decomposition of the LATP plate in aqueous LiOH and aqueous HCl as confirmed from the XRD study and the SEM observation. Fig. 7 shows the temperature dependence of the electrical conductivity of the pristine LATP plate and the LATP plated immersed for 3 weeks in aqueous 1 M $LiNO_3$. The bulk conductivity slightly decreased, while the grain boundary conductivity increased. These changes come from a fitting condition of the impedance profiles. The total electrical conductivity of the LAPT plate is the same both before and after the immersion. The LATP plate immersed in aqueous 1 M LiCl exhibited no conductivity change within 3 weeks. The existence of Li^+ ions may contribute to the stability of the LATP plate in the presence of water. The second phase observed in the LAPT plate immersed in distilled water may be due to the ionic exchange reaction between Li^+ and H^+, and the reaction may be suppressed by the presence of Li^+ ions.

The water stability test for the lithium/air cell with the LATP plate electrolyte was carried out in aqueous 1 M LiCl. Fig. 8 shows the impedance profiles of the Li–Al/LiPON/LATP/LiPON/Li–Al symmetrical cell and the Li–Al/LiPON/LATP/aqueous 1 M LiCl/Pt cell at

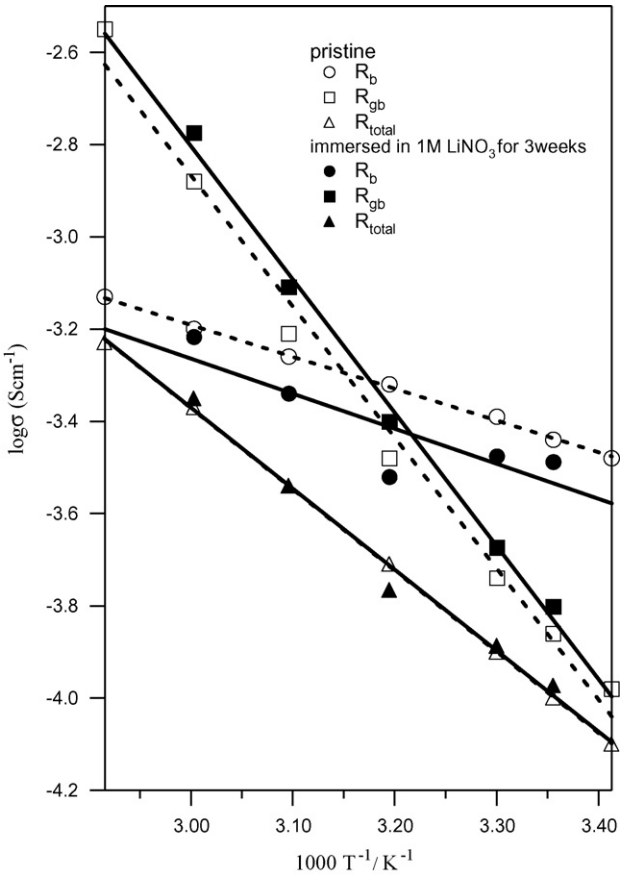

Fig. 7. Temperature dependence of total conductivity, grain conductivity, and grain boundary conductivity of the LATP plate immersed in 1 M $LiNO_3$ for 3 weeks.

40 °C. The cell resistance of Li–Al/LiPON/LATP/aqueous 1 M LiCl/Pt is estimated 3100 Ω, which is almost half the resistance of 8000 Ω for Li–Al/LiPON/LATP/LiPON/Li–Al. The major component of the cell resistance of the latter symmetrical cell comes from the interface resistance between Li–Al/LiPON [10]. Therefore, it is suggested here that the interfacial resistance of the LATP plate and the aqueous LiCl solution may be quite low. Hence, the lithium ion transport between the LATP solid electrolyte and the liquid electrolyte is fast enough. Fig. 9 shows the time dependence of the impedance profiles of the Li–Al/LiPON/LATP/aqueous 1 M LiCl/Pt at 25 °C. The cell resistance slightly increased from 8300 to 10,000 Ω after 3 days and then decreased to 7200 Ω after 7 days. The reason for this resistance change is not clear, but the impedance profiles after 1 week storage are almost the same as that of the initial cell. This means that the Li–Al/LiPON/LATP is stable even in water, and that the water does not penetrate through the LATP plate.

Fig. 10 shows a constant current (30 μA cm^{-2}) discharge curve at 25 °C. The open circuit voltage (OCV) of the Li–Al/LiPON/LATP/aqueous 1 M LiCl/Pt was 3.6 V at 25 °C, and was stable for 1 week. The theoretical OCV value calculated from the following reaction

$$2Li + (1/2)O_2 + H_2O = 2LiOH$$

is 3.8 V. Thus, the observed OCV is slightly lower than the calculated one. The low OCV may be due to the effect of a small amount of Al in the Li electrode, and/or the low oxygen partial pressure on the Pt electrode. The initial cell resistance was estimated to be 8000 Ω from the current and cell voltage curve, which is comparable to the total cell resistance observed by ac impedance profiles. The decrease of the cell voltage may be due to polarization between the

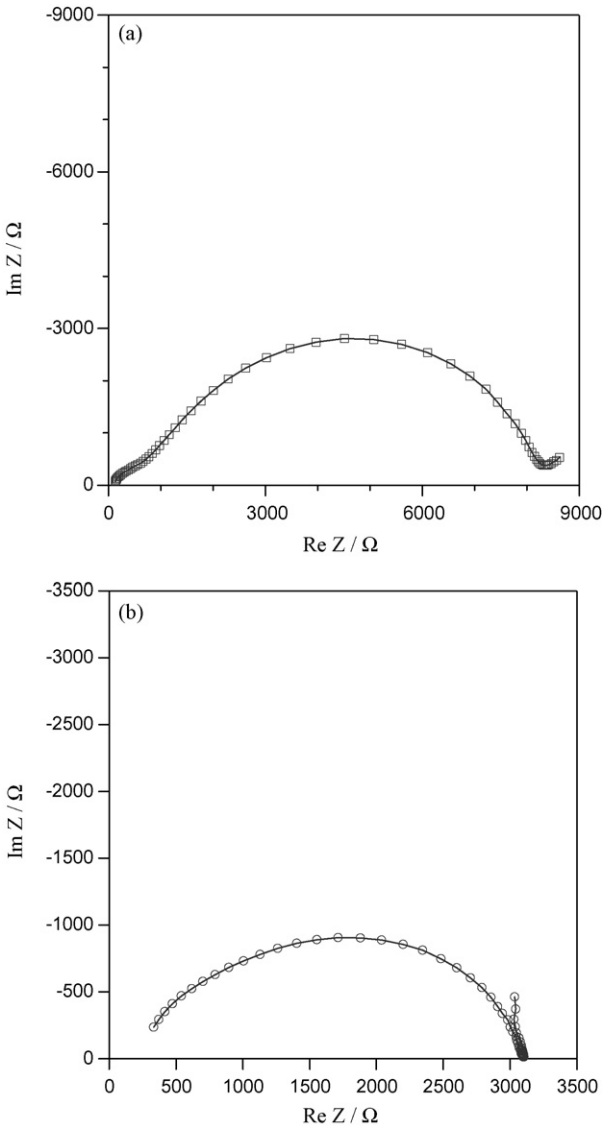

Fig. 8. Impedance spectra at 40 °C of Li–Al/LiPON/LATP/LiPON/Li–Al cell (a) and Li–Al/LiPON/LATP/1 M LiCl/Pt cell (b).

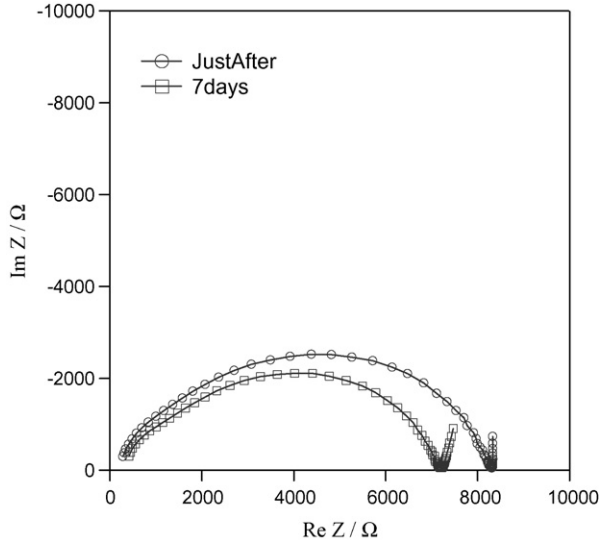

Fig. 9. Impedance spectra change with time of Li–Al/LiPON/LATP/1 M LiCl/Pt at 25 °C.

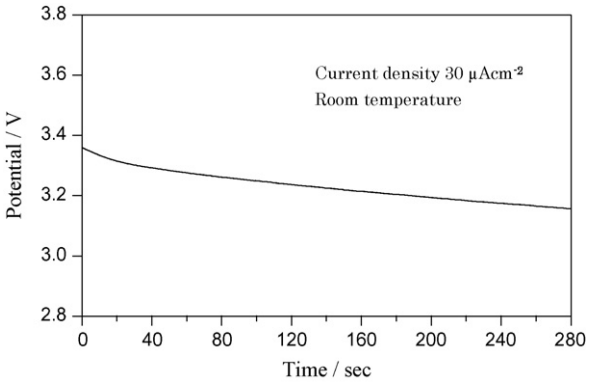

Fig. 10. Constant current ($30\,\mu A\,cm^{-2}$) discharge performance of Li–Al/LiPON/LATP/1 M LiCl/Pt at 25 °C.

Li metal anode and LiPON. From a practical applications standpoint for the lithium/air batteries, the interfacial resistance between the lithium metal and LiPON should be reduced, which is subject of work currently underway.

4. Conclusions

The water stability of the NASICON-type lithium ion conducting solid, $Li_{1+x+y}Al_xTi_{2-x}P_{3-y}Si_yO_{12}$ (LATP), for the electrolyte in the lithium/air battery was examined in various types of aqueous solution. The LATP plate was stable in aqueous 1 M $LiNO_3$ and aqueous 1 M LiCl. The LATP immersed in aqueous HCl and LiOH showed a high resistance. The LATP plate immersed in aqueous 1 M LiOH decomposed, and $LiPO_4$ appeared as a result. In distilled water containing no electrolyte salt, the electrical conductivity of the LATP plate slightly increased with immersion period, and the impedance profile suggested that a new phase occurred at the grain boundary. The Li–Al/LiPON/LATP/aqueous 1 M LiCl/Pt cell showed a stable OCV of 3.6 V at 25 °C for 1 week. The interfacial resistance between the LATP solid electrolyte and the aqueous LiCl solution was low. To obtain a high performance lithium/air battery, the interfacial resistance between the lithium electrode and the LiPON layer should be reduced.

Acknowledgments

We thank OHARA Inc. for supplying the LATP plate and powder and are grateful to Dr Y. Inda of OHARA Inc. for the helpful comments and suggestions.

This research was sponsored by the New Energy and Industrial Technology Development Organization (NEDO) of Japan under the project, Development of High Performance Battery System for Next-Generation Vehicles.

References

[1] J. Read, J. Electrochem. Soc. 149 (2002) A1190–1195.
[2] T. Ogasawara, A. Debart, M. Holzapfel, P. Novak, P.G. Bruce, J. Am. Chem. Soc. 128 (2006) 1390–1393.
[3] K.M. Abraham, Z. Jiang, J. Electrochem. Soc. 143 (1996) 1–5.
[4] S.J. Visco, E. Nimon, B. Katz, L.C.D. Jonghe, M.Y. Chu, IMLB vol. 12, 2004, Abstract #53.
[5] T. Kuboki, T. Okuyama, T. Ohsaki, N. Takami, J. Power Sources 146 (2005) 766–769.
[6] S.J. Visco, E. Nimon, B. Katz, L.C.D. Jonghe, M.Y. Chu, 210th ECS Meeting, 2006, Abstract #389.
[7] H. Aono, E. Sugimoto, Y. Sadaoka, N. Imanaka, G. Adachi, J. Electrochem. Soc. 136 (1989) 590–591.
[8] M. Cretin, P. Fabry, L. Abello, J. Eur. Ceram. Soc. 15 (1995) 1149–1156.
[9] J.S. Thokchom, B. Kumar, J. Electrochem. Soc. 154 (2007) A331–A336.
[10] N. Imanishi, S. Hasegawa, T. Zhang, A. Hirano, Y. Takeda, O. Yamamoto, J. Power Sources, in press.
[11] J. Fu, Solid State Ionics 96 (1997) 195–200.
[12] J. Fu, US Patent 5,702,995 (1997).
[13] P.G. Bruce, A.R. West, J. Electrochem. Soc. 130 (1983) 662–669.